AerospaceEurope Conference2021
WARSAW, POLAND | 23 -26 NOVEMBER 2021
CEAS Council of European Aerospace Societies

PREDICTION OF AIRFOIL TONAL NOISE USING URANS COMPUTATIONS AND ITS MITIGATION

Witold Klimczyk, Adam Sieradzki & Paweł Kękuś-Kumor

Aerodynamics Department, Łukasiewicz Research Network - Institute of Aviation, Warsaw, Poland

Abstract

Laminar boundary layer vortex shedding is one of the main sources of airfoil self-noise. It occurs at moderate Reynolds numbers and angles of attack, where a relatively large region of laminar boundary layer is developed over an airfoil. The airfoil tonal noise, which is a result of laminar boundary layer instabilities, is critical in designing low-noise airfoils. The identification of tones and calculation of noise levels require a high-fidelity aerodynamic model, capable of resolving the laminar boundary layer, accurately predicting the transition region, formation of instabilities and their propagation downstream. Whereas the typical computational aeroacoustics (CAA) procedures require scale-resolving simulations, the aforementioned physics may be as well captured using the unsteady RANS model. Current work presents the approach to modeling of tonal noise using relatively cheap URANS simulations. The general case of asymmetric S834 airfoil was investigated at Reynolds number of 5×10^5. Hence, the tonal noise mitigation was performed using zigzag tape to trip the boundary layer. A hybrid aeroacoustic approach using Lighthill analogy was adopted to calculate noise levels for both cases, which compared to experimental results from the literature confirmed the usefulness of the presented approach. The vital aspects of creating CFD URANS model capable of capturing tonal noise at correct frequency were examined by comparison to experimental data from literature. The most significant aspect involved mesh generation, with unstructured, low aspect-ratio meshes allowing the most reliable solution. The existence of tonal noise in clean airfoil case and effectiveness of zigzag tape in tones prevention was correctly modeled with URANS. This is especially important in the context of airfoil design and optimization, infeasible if typical, expensive scale-resolving approach is considered.

Keywords: Airfoil noise, CAA, CFD

1. Introduction

Ever-increasing importance of aerodynamic noise is a result of recent emergence of, amongst others, wind turbines, multirotor unmanned (and potentially manned) vehicles. Especially the omnipresence of the latter, with prospects of incorporation of multirotor transport in the densely populated urban areas [2], requires the effective solutions to aerodynamic noise mitigation. Whereas the propeller noise is typically addressed by analysis of thickness and loading constituents, the influence of airfoil shape and related airfoil self-noise cannot be neglected.
Airfoil self-noise is typically divided into five types [3]:

1. Turbulent boundary layer (TBL) trailing edge noise, where the noise is generated as turbulence passes over the trailing edge. Typically results in broadband noise spectrum.

2. Laminar boundary layer (LBL) vortex shedding (VS) instability noise, which occurs for low Reynolds number and low turbulence flows. Laminar instabilities generated on the laminar bubble develop vortices responsible for high levels of tonal noise, which is schematically depicted in Figure 1.

3. Boundary layer separation (BLS), which generates noise due to shed turbulent vorticity. Increasing angle of attack shifts position of separation towards the leading edge, resulting in deep stall, which in turn generates low-frequency noise.

4. Blunt trailing edge (BTE) noise is caused by vortex shedding behind the thick trailing edge.

5. Tip vortex noise, resulting from highly turbulent flow occurring near the tips of lifting blades or wings.

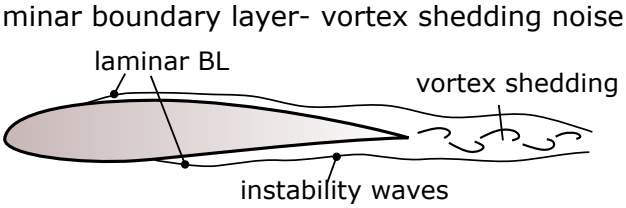

Figure 1 – Schematic view of airfoil LBL-VS self-noise.

In the current work second type of noise is considered, i.e. LBL-VS noise.

LBL-VS physics One of the first comprehensive works on the airfoil tonal noise was performed experimentally in 1970's [17]. The 'ladder-type' variation of the peak tone frequency f_s was obtained, relating it to free-stream flow speed u_∞, airfoil chord c and air kinematic viscosity ν: $f_s = 0.011 u_\infty^{1.5} (c\nu)^{-0.5}$. The self-excited aeroacoustic feedback was soon proposed [20], which assumes the tonal noise is due to the first instability excited by a point downstream. This idea was further investigated, so that the aeroacoustic signal was assumed to originate at the airfoil trailing edge as a result of Tollmien-Schlichting (T-S) waves diffraction. T-S waves are in turn triggered by acoustic signal, which closes the feedback loop [1]. The validity of aeroacoustic feedback theory was discussed [13], concluding that the feedback is not necessary for tonal noise to occur. It was found that the tonal noise is largely dependent on the separation bubble existence. [12] established that the tones appear only up to a limited angle of incidence and in certain Reynolds number range. Some more recent attempts can be found in e.g. [18], which generally confirms the separation bubble importance on the tonal noise and the tones existence conditions.
In the light of these findings, LBL-VS is potentially important in the context of low Reynolds number propellers, which operate in low turbulence conditions and at moderate angles of attack. Additionally, an appropriate computational model must be selected, which allows to identify the existence of tonal noise on arbitrary airfoil, with the associated cost not ruling out the shape optimization.

CFD for acoustics The computational analysis of airfoil noise, especially if broadband noise is considered, requires high-fidelity aerodynamic model, capable of resolving scales of turbulence, such as the Large Eddy Simulation (LES) [7] or hybrid RANS-LES [14]. The tonal nature of LBL-VS noise requires appropriate modeling of laminar-turbulent boundary layer transition and formation of laminar instabilities, which propagate over the airfoil surface up to the trailing edge. Especially late transition, occurring at low turbulence conditions is important. The complexity of LBL-VS further increased by the aeroacoustic feedback from the airfoil trailing edge, responsible for amplification of T-S waves, requires direct CAA methods performed with Direct Numerical Simulations (DNS) [19, 6]. While direct CAA resolve the acoustic field, the tonal noise existence and levels can be modeled with good accuracy using relatively cheap unsteady RANS model [5] with transition SST used for turbulence closure.
Examples of tonal noise reduction strategies are primarily concentrated on eliminating laminar boundary layer, using e.g.: LE sinusoidal modifications [8], trailing edge serrations [4], boundary layer tripping [16]. The latter is selected in the current study to test the cheap RANS model.
In practical engineering applications, where the goal is to design quiet and well-performing propeller, the use of high-fidelity CFD (such as DNS, or even LES) is often not feasible due to the computational

cost. Especially where the use of optimization is required, and the potential number of cases to be computed is of the order of hundreds, the cheap and robust way of obtaining the information regarding airfoil tonal noise is necessary. Current work is concentrated on development of a cheap method, capable of capturing the tonal airfoil self-noise component, which can be used for example for qualitative optimization. The focus is on LBL-VS noise modeling, specifically on obtaining an aerodynamic model sufficient to capture the tones as well as ensure the tones are not present.
In section 2, the aerodynamic model is described, including study of different meshing approaches (e.g. structured/unstructured). Hence, in section 3 the acoustic analysis using Lighthill analogy is described. The findings of current study are then summarized in section 4.

2. Aerodynamics modeling

Viscous fluid motion is described by Navier-Stokes (N-S) equations, i.e. continuity equation:

$$\frac{\partial \rho}{\partial t} + \nabla \cdot (\rho \vec{u}) = 0, \tag{1}$$

and momentum conservation equations:

$$\frac{\partial}{\partial t}(\rho \vec{u}) + \nabla \cdot (\rho \vec{u}\vec{u}) = -\nabla p + \nabla \cdot (\bar{\bar{\tau}}) \tag{2}$$

where p is static pressure, $\bar{\bar{\tau}}$ is the stress tensor, defined as:

$$\bar{\bar{\tau}} = \mu \left[\left(\nabla \vec{u} + \nabla \vec{u}^T \right) - \frac{2}{3} \nabla \cdot \vec{u} I \right], \tag{3}$$

where μ is the molecular viscosity, I is the unit tensor.
Direct numerical solution of N-S equations is extremely costly and is generally not performed in practical engineering applications. The most popular simplification of N-S equations in industrial practice involves averaging, which results in Reynolds-Averaged Navier-Stokes (RANS).
RANS equations are of the form:

$$\frac{\partial \rho}{\partial t} + \frac{\partial}{\partial x_i}(\rho u_i) = 0, \tag{4}$$

$$\frac{\partial}{\partial t}(\rho u_i) + \frac{\partial}{\partial x_j}(\rho u_i u_j) = -\frac{\partial p}{x_i} + \frac{\partial}{\partial x_j}\left[\mu \left(\frac{\partial u_i}{\partial x_j} + \frac{\partial u_j}{\partial x_i} - \frac{2}{3}\delta_{ij}\frac{\partial u_k}{\partial x_k} \right) \right] + \frac{\partial}{\partial x_j}\left(-\rho \overline{u_i' u_j'} \right) \tag{5}$$

The fluctuating term $-\rho \overline{u_i' u_j'}$ is the Reynolds stress term. Additional modeling is required to close RANS equations. Eddy viscosity models relate Reynolds stresses to the mean velocity gradients:

$$-\rho \overline{u_i' u_j'} = \mu_t \left(\frac{\partial u_i}{\partial x_j} + \frac{\partial u_j}{\partial x_i} \right) - \frac{2}{3}\left(\rho k + \mu_t \frac{\partial u_k}{\partial x_k} \right) \delta_{ij}. \tag{6}$$

CFD setup To address the problem strongly dependent upon correct prediction of laminar-turbulent boundary layer transition, the transition-SST RANS model [15] was used for turbulence closure. This model has been shown to allow very precise transition prediction [9]. Computations were performed using commercial code *Ansys Fluent*. Incompressible pressure-based solver was selected due to low freestream velocity ($u_\infty < 0.1M$). Firstly, a steady RANS solution was calculated using coupled pressure-velocity solver, then for unsteady solution non-iterative time advancement and fractional step scheme was used. A bounded second order implicit scheme was used for temporal discretization. Least squares cell-based method was used to calculate gradients. Pressure was discretized using second order scheme, while the second order upwind scheme was used for momentum, k, ω, γ and Re_θ. Courant-Friedrichs-Lewy (CFL) number was strictly below 1 everywhere in the domain, with maximum $CFL \simeq 0.2$ in the region of laminar instabilities formation (i.e. in the outer part of prisms zone). For the final mesh the time step $dt = 1 \times 10^{-6}$. Case setup was defined to recreate the experiment described in the literature [16]. The key characteristics of the analysis are summarized in Tab. 1.

Table 1 – Case summary.

u_∞	$32\ [m/s]$
ρ	$1.225\ [kg/m^3]$
Re	$5 \times 10^5\ [-]$
α	$4.4\ [^\circ]$
c	$0.2286\ [m]$
Turb. intensity	0.06%
Turb. model	Transition SST (4 eq.)

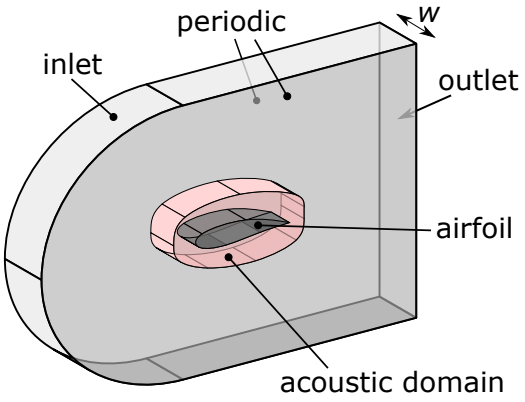

Figure 2 – Schematic view of 2.5D CFD domain setup.

2.1 CFD mesh independence study

As the current study was aimed to perform aeroacoustic analysis, the influence of mesh in the acoustic sources domain was investigated. Whereas the typical mesh independence study is performed to assure lift and drag convergence to a certain tolerance, current study was additionally aimed to find mesh sufficient to qualitatively and quantitatively capture vortex shedding. The mesh refinement study accounted for both unstructured volume mesh parameters, as well as surface mesh sizing and the number and growth rate of prism layers. The volume refinement region in the rear part of the airfoil was added, to ensure local grid refinement in the region of expected vortex shedding. Prism layers were established to capture the whole boundary layer, especially in the vicinity of laminar instabilities formation region. Table 2 presents the summary of mesh independence study. It was noted that the base mesh was unable to capture the laminar instabilities, and further refinement of near wall region was required. Importantly, if the independence study was to be based on pure force convergence it would likely accept mesh 1 as sufficiently accurate. With more prism layers and/or finer volume mesh outside of prisms, the instabilities were captured. Two approaches were compared—polyhedral-hexcore with less prisms and finer volume mesh (mesh 2), and pure polyhedral with more prisms but larger volume mesh size (mesh 3). The latter approach allowed to resolve laminar instabilities, which result in higher forces oscillations and further refinement of this mesh type was investigated (mesh 4). As no major difference was observed, mesh 3 was deemed sufficient for current analysis. Figures 3 and 4 present the mesh on the mid-plane showing the refined regions and level of refinement.
Apart from the unstructured mesh, the structured 2-dimensional approach was considered. It was found, that the flow pattern was slightly different, with laminar instabilities developing on both sides of an airfoil. As a result, the frequency of force oscillations was significantly different to the experiment, and the structured approach was abandoned.

2.2 Results

Visualization of laminar instabilities-triggered vortex shedding is presented in Figure 5 using q-criterion iso-surfaces. It can be observed, that the quasi two-dimensional vortices are triggered in the area of laminar-turbulent transition and propagate downstream, past trailing edge into airfoil wake. The same q-criterion for airfoil with a trip in Figure 6 shows that no vortices are created.

Table 2 – Mesh independence study summary.

Mesh	Mean c_l	Mean c_d	Frequency	Amplitude (c_l)
1- base	0.6903	0.009268	-	0
2- poly-hex	0.6950	0.009217	1648	0.00046
3- poly1	0.6943	0.009218	1646	0.00078
4- poly2	0.6932	0.009219	1663	0.00061

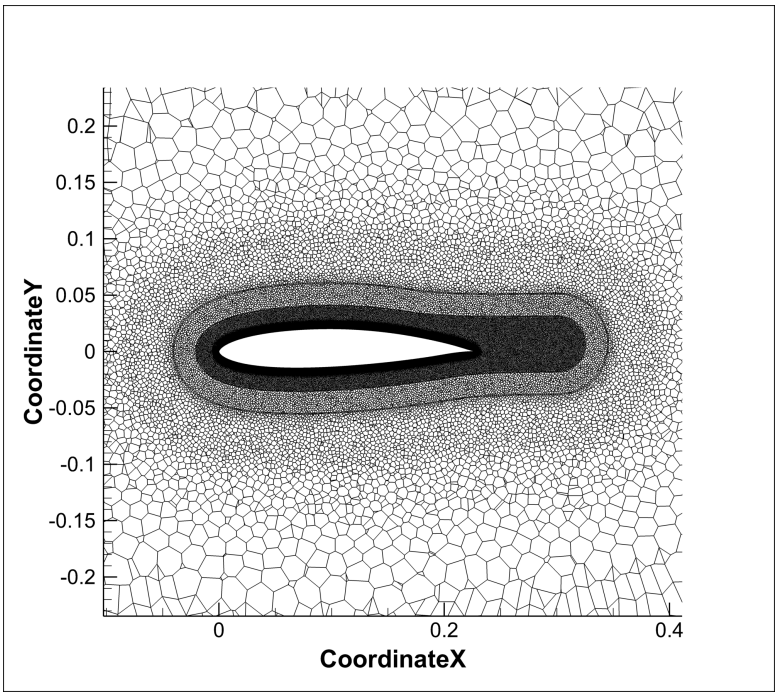

Figure 3 – View on the airfoil mesh with surrounding domains. The refined acoustic sources zone includes region surrounding airfoil and is extended to capture wake.

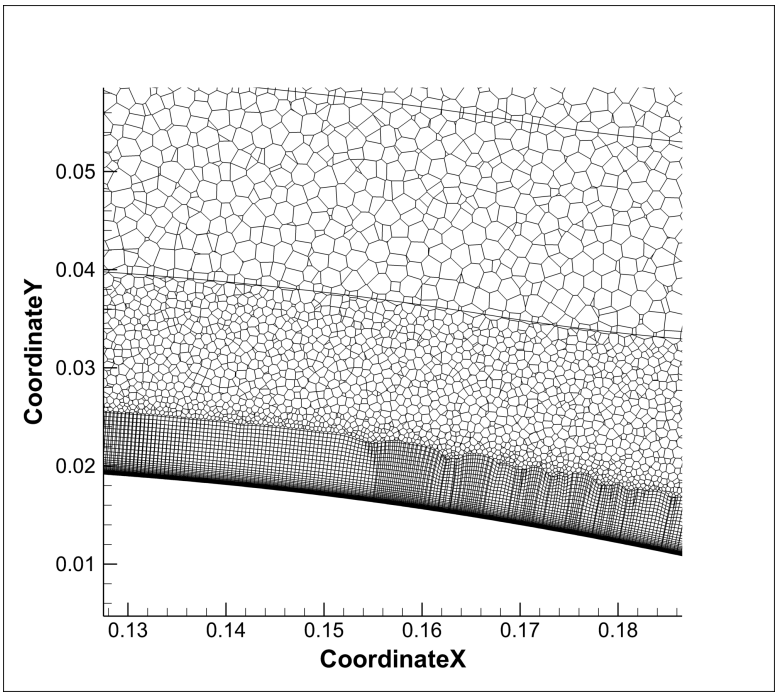

Figure 4 – Close-up on near wall mesh.

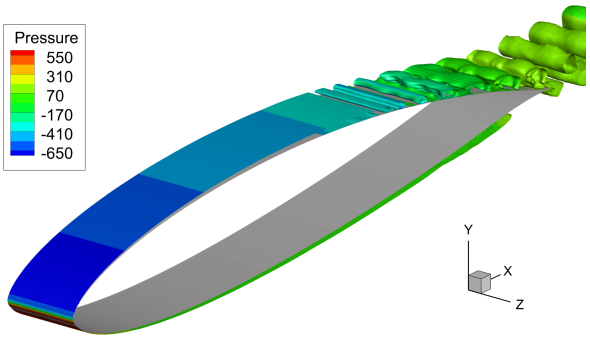

Figure 5 – Q-criterion iso-surfaces show the LBL-VS pattern.

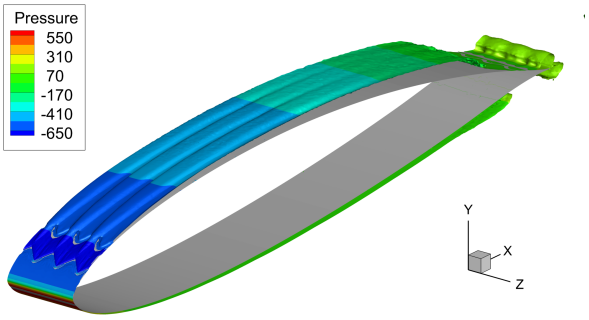

Figure 6 – Airfoil with trip prevents vortex shedding.

Pressure coefficient (c_p) on the airfoil surface is presented in Figure 7. The time-averaged and instantaneous values show the effect of laminar instabilities downstream of laminar-turbulent transition. Even though the oscillations are damped towards the trailing edge, the tones are still present and result in tonal noise.

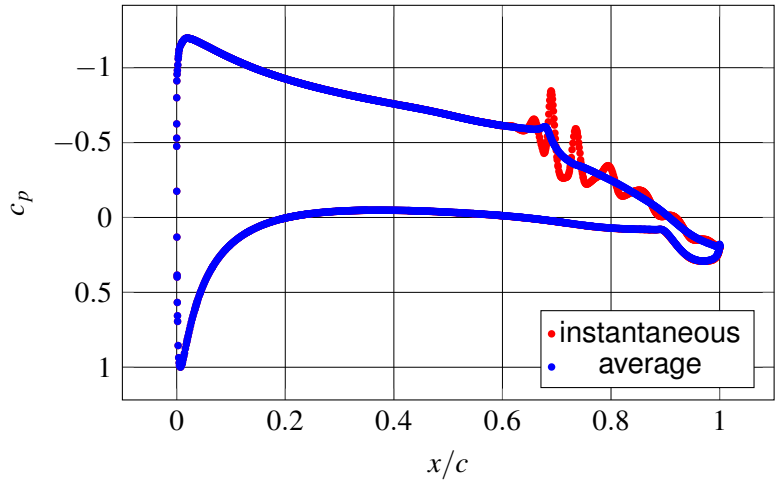

Figure 7 – Pressure coefficient on the clean S834 airfoil surface, instantaneous and average values.

The effect of trip on the aerodynamics is presented in Figures 8 and 9. It can be observed, that the turbulent intensity is significantly increased directly downstream of zigzag tape position. As a result, the transition to turbulence occurs much earlier and the formation of laminar instabilities is prevented.

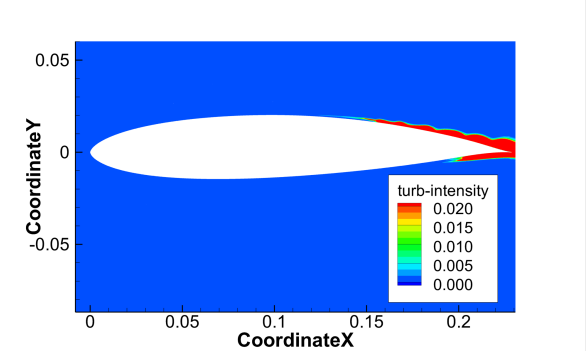

Figure 8 – Turbulent intensity for clean airfoil. The increase is observed after laminar-turbulent transition.

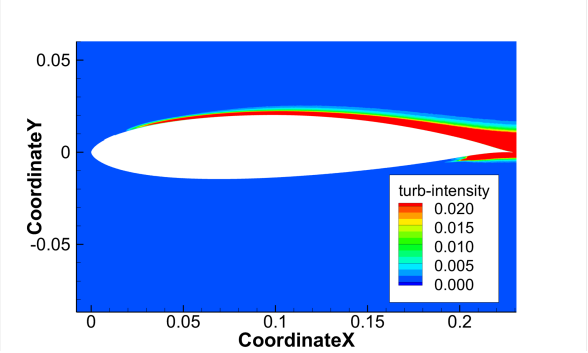

Figure 9 – Turbulent intensity for airfoil with trip. Turbulence level over the airfoil is significantly higher.

3. Acoustics analysis

3.1 Lighthill analogy based noise calculations

Due to the computational cost of direct aeroacoustic computations, the acoustic analogy approach was used in current work. The separation of acoustic and flow dynamics allows to propagate the noise from sources to receivers surrounding the object of interest, hence calculate the sound pressure levels at required locations. Lighthill's analogy [10, 11] is formulated by rearranging Navier-Stokes equations with acoustic density perturbation $\rho' = \rho - \rho_0$:

$$\frac{\partial^2 \rho'}{\partial t^2} - c_0 \frac{\partial^2 \rho'}{\partial x_i \partial x_i} = \frac{\partial^2 T_{ij}}{\partial x_i \partial x_j}, \tag{7}$$

where the left side of equation describes propagation operator for all regions of domain and right side describes equivalent acoustic source. It is described for source region only and is based on the Lighthill tensor T_{ij} approximation for low Mach, incompressible flow:

$$T_{ij} \approx \rho u_i u_j, \tag{8}$$

i.e. sources are calculated from velocity fluctuations. Whereas the solution in the source region is typically discarded due to limited accuracy, the calculated acoustic far-field is accurate. Lighthill analogy can only be used in low freestream velocity conditions. It assumes that no acoustic sources are present in the far-field, which puts restrictions on the definition of source region.

In the current work, Lighthill analogy, with volume sources in the region surrounding airfoil was used. The analysis was performed using a commercial software *Actran*. Firstly, aeroacoustic sources were computed from unsteady CFD results and transformed to frequency domain. Hence, the finite element method-based solver was used to calculate acoustic pressure propagation in the acoustic domain. 1/3 octave band sound pressure levels were calculated at microphones surrounding the trailing edge at a distance of $0.63m$ (as in the experiment). The acoustic mesh was of the same width as CFD mesh, and was extended up to the microphones location. This allows reflection of sound waves from sides of the acoustic domain, which corresponds to an infinite-span wing. The non-reflecting boundary was used on the surface surrounding the domain. The acoustic analysis domain setup is schematically presented in Figure 10. The acoustic mesh is presented in Figure 11.

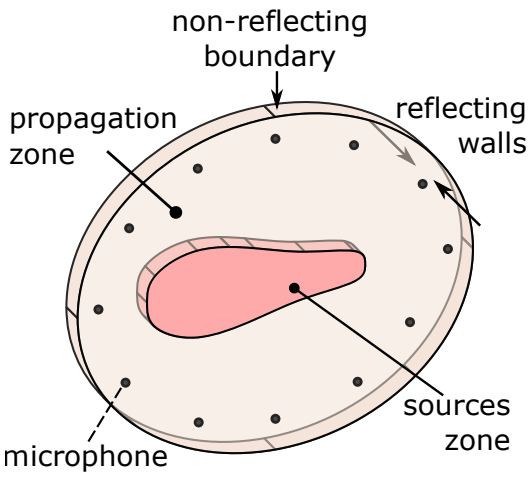

Figure 10 – Schematic view of the acoustic domain setup.

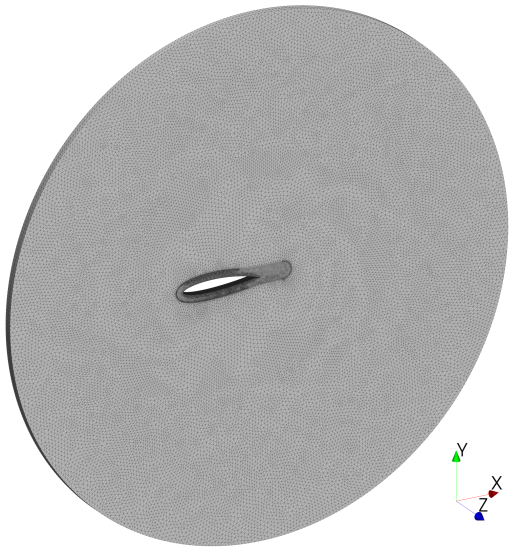

Figure 11 – Acoustic mesh.

3.2 Results

For comparison with experiment, SPL values at microphones were converted to sound power level (PWL), assuming full spherical space, i.e.:

$$PWL = SPL - 10\log\left[\frac{1}{4\pi \times 0.63^2}\right]. \tag{9}$$

The 1/3 octave band PWL is presented in Figure 12 for both clean and trip cases, for a microphone located directly above the trailing edge. The experimental data from literature [16] is plotted for comparison. Tonal peak can be observed for clean airfoil at $f = 1600Hz$, which corresponds to the frequency of lift and drag oscillations found in CFD. The difference in PWL is most likely resulting from slightly different flow conditions in experiment and CFD, e.g. in turbulence properties. Additionally, the computational model was used to calculate noise from infinite wing as opposed to finite wing in the experiment. Calculated PWL for airfoil with trip is very low, with values above $20dB$ only in the range $1000 - 1600Hz$. This indicates some relatively little flow oscillations captured by URANS model.

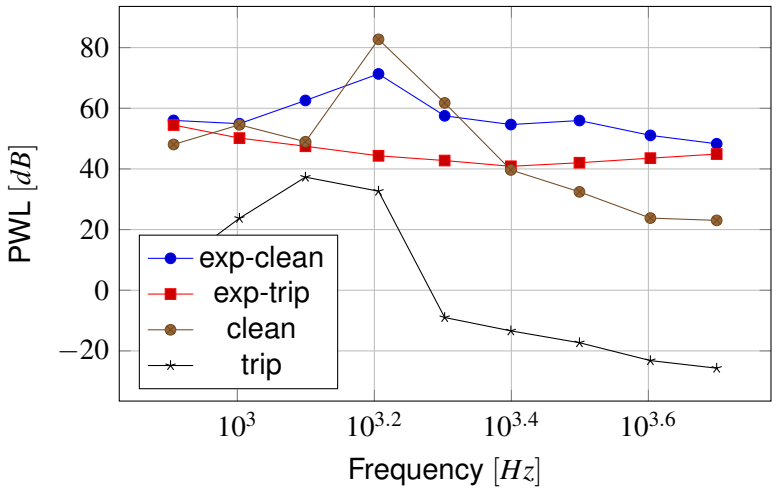

Figure 12 – PWL comparison of clean and trip airfoils, along with experimental data from literature [16].

Acoustic pressure map for the peak tone frequency $f = 1600Hz$ is presented in Figure 13. Pressure oscillations are present on the pressure side of an airfoil (as computed by URANS), as well as in its wake. The wake was resolved only up to certain point, defined by the sources region. Importantly, the main noise source is located at the airfoil trailing edge. The amplitude of acoustic pressure fluctuations varies and is the lowest upstream and downstream of the airfoil. The highest fluctuations are observed above the suction side of the airfoil, which is consistent with experiment [16].

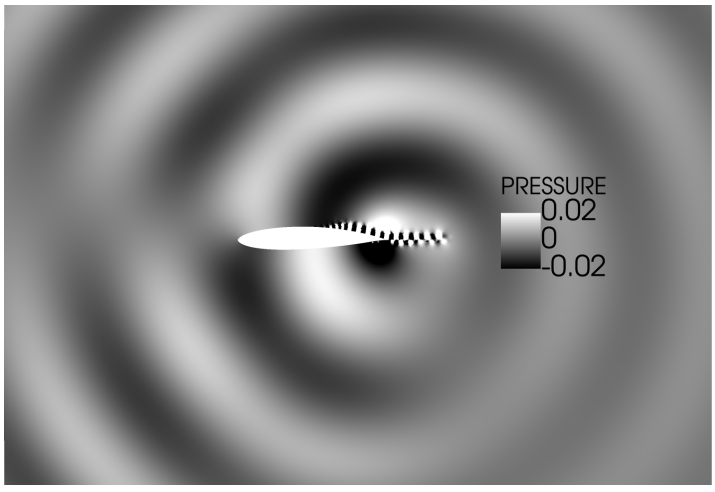

Figure 13 – Acoustic pressure around the airfoil at the peak tone frequency $f = 1600Hz$.

The acoustic analyses based on the URANS CFD were expected to confirm the existence of tonal noise for clean airfoil, and lack of tones for airfoil with trip. It can be concluded that the presented approach is sufficient in identification of tonal noise existence. If more details, especially regarding the broadband noise are required, scale-resolving simulation must be performed. This is especially important in case of an airfoil with trip, where the trip-initiated turbulence build-up results in high

frequency noise.

4. Summary

A successful attempt to model the tonal noise of a generic, asymmetric airfoil with late transition to turbulent boundary layer using URANS has been performed. The sensitivity of URANS model to mesh type and freestream conditions was examined. It was found, that the low aspect-ratio, unstructured mesh with fine near-wall mesh is required to resolve laminar instabilities and resulting vortex shedding. The noise calculations using Lighthill analogy were performed to find the tonal noise levels in 1/3 octave bands. The comparison with experiment revealed some differences regarding PWL at peak frequency, which is a result of non-exact recreation of experiment. Specifically, the finite wing PWL from experiment was compared to infinite wing PWL from computational model. Moreover, the experiment freestream conditions were described with limited accuracy, which prevented exact recreation in CFD.

The limitations of URANS for prediction of airfoil tonal noise existence are related to lack of modeling of the aeroacoustic feedback. Current study showed, that the correct prediction of laminar instabilities and their frequency can be performed without consideration of the feedback loop. Future considerations extending current work include scale-resolving simulation to calculate the broadband noise, especially in the case of an airfoil with trip.

Acknowledgements

This work has been supported by the Interdisciplinary Centre for Mathematical and Computational Modelling (ICM), University of Warsaw (UW), within grant no G84-19.

References

[1] Henri Arbey and J Bataille. “Noise generated by airfoil profiles placed in a uniform laminar flow”. In: *Journal of Fluid Mechanics* 134 (1983), pp. 33–47.

[2] Paul Bent et al. “Urban Air Mobility Noise: Current Practice, Gaps, and Recommendations”. In: (2020).

[3] Thomas F Brooks, D Stuart Pope, and Michael A Marcolini. *Airfoil self-noise and prediction*. Vol. 1218. National Aeronautics and Space Administration, Office of Management . . ., 1989.

[4] Tze Pei Chong et al. “Self-noise produced by an airfoil with nonflat plate trailing-edge serrations”. In: *AIAA journal* 51.11 (2013), pp. 2665–2677.

[5] Michele De Gennaro, Helmut Kühnelt, and Alessandro Zanon. “Numerical prediction of the tonal airborne noise for a NACA 0012 aerofoil at moderate Reynolds number using a transitional URANS approach”. In: *Archives of Acoustics* 42.4 (2017), pp. 653–675.

[6] G Desquesnes, M Terracol, and P Sagaut. “Numerical investigation of the tone noise mechanism over laminar airfoils”. In: *Journal of Fluid Mechanics* 591 (2007), pp. 155–182.

[7] Marshall Galbraith and Miguel Visbal. “Implicit large eddy simulation of low Reynolds number flow past the SD7003 airfoil”. In: *46th AIAA aerospace sciences meeting and exhibit*. 2008, p. 225.

[8] Kristy Hansen, Richard Kelso, and Con Doolan. “Reduction of flow induced airfoil tonal noise using leading edge sinusoidal modifications”. In: *Acoustics Australia* 40.3 (2012), pp. 172–177.

[9] Robin Blair Langtry et al. “A correlation-based transition model using local variables—part II: test cases and industrial applications”. In: (2006).

[10] Michael James Lighthill. “On sound generated aerodynamically I. General theory”. In: *Proceedings of the Royal Society of London. Series A. Mathematical and Physical Sciences* 211.1107 (1952), pp. 564–587.

[11] Michael James Lighthill. “On sound generated aerodynamically II. Turbulence as a source of sound”. In: *Proceedings of the Royal Society of London. Series A. Mathematical and Physical Sciences* 222.1148 (1954), pp. 1–32.

[12] Martin Lowson, Steven Fiddes, and Emma Nash. “Laminar boundary layer aero-acoustic instabilities”. In: *32nd Aerospace Sciences Meeting and Exhibit*. 1994, p. 358.

[13] Alan McAlpine, EC Nash, and MV Lowson. “On the generation of discrete frequency tones by the flow around an aerofoil”. In: *Journal of Sound and Vibration* 222.5 (1999), pp. 753–779.

[14] Florian Menter et al. “An overview of hybrid RANS–LES models developed for industrial CFD”. In: *Applied Sciences* 11.6 (2021), p. 2459.

[15] Florian R Menter et al. “A correlation-based transition model using local variables—part I: model formulation”. In: (2006).

[16] Stefan Oerlemans and P Migliore. “Wind tunnel aeroacoustic tests of six airfoils for use on small wind turbines”. In: *Report of the National Renewable Energy Laboratory NREL/SR-500-35339* (2004).

[17] Robert W Paterson et al. “Vortex noise of isolated airfoils”. In: *Journal of Aircraft* 10.5 (1973), pp. 296–302.

[18] S Pröbsting, J Serpieri, and F Scarano. “Experimental investigation of aerofoil tonal noise generation”. In: *Journal of Fluid Mechanics* 747 (2014), pp. 656–687.

[19] RD Sandberg et al. “Direct numerical simulations of tonal noise generated by laminar flow past airfoils”. In: *Journal of Sound and Vibration* 320.4-5 (2009), pp. 838–858.

[20] Christopher KW Tam. “Discrete tones of isolated airfoils”. In: *The Journal of the Acoustical Society of America* 55.6 (1974), pp. 1173–1177.